

# Hosing of a long relativistic particle bunch in plasma

T. Nechaeva,<sup>1,\*</sup> L. Verra,<sup>2</sup> J. Pucek,<sup>1</sup> L. Ranc,<sup>1</sup> M. Bergamaschi,<sup>1</sup> G. Zevi Della Porta,<sup>1,2</sup> and P. Muggli<sup>1</sup>  
(AWAKE Collaboration)

R. Agnello,<sup>3</sup> C.C. Ahdida,<sup>2</sup> C. Amoedo,<sup>2</sup> Y. Andrebe,<sup>3</sup> O. Apsimon,<sup>4,5</sup> R. Apsimon,<sup>5,6</sup> J.M. Arnesano,<sup>2</sup>  
V. Bencini,<sup>2,7</sup> P. Blanchard,<sup>3</sup> P.N. Burrows,<sup>7</sup> B. Buttenschön,<sup>8</sup> A. Caldwell,<sup>1</sup> M. Chung,<sup>9</sup> D.A. Cooke,<sup>10</sup>  
C. Davut,<sup>4,5</sup> G. Demeter,<sup>11</sup> A.C. Dexter,<sup>5,6</sup> S. Doebert,<sup>2</sup> J. Farmer,<sup>1</sup> A. Fasoli,<sup>3</sup> R. Fonseca,<sup>12,13</sup> I. Furno,<sup>3</sup>  
E. Granados,<sup>2</sup> M. Granetzny,<sup>14</sup> T. Graubner,<sup>15</sup> O. Grulke,<sup>8,16</sup> E. Gschwendtner,<sup>2</sup> E. Guran,<sup>2</sup> J. Henderson,<sup>5,17</sup>  
M.Á. Kedves,<sup>11</sup> S.-Y. Kim,<sup>9,2</sup> F. Kraus,<sup>15</sup> M. Krupa,<sup>2</sup> T. Lefevre,<sup>2</sup> L. Liang,<sup>4,5</sup> S. Liu,<sup>18</sup> N. Lopes,<sup>13</sup> K. Lotov,<sup>19,20</sup>  
M. Martinez Calderon,<sup>2</sup> S. Mazzoni,<sup>2</sup> K. Moon,<sup>9</sup> P.I. Morales Guzmán,<sup>1</sup> M. Moreira,<sup>13</sup> N. Okhotnikov,<sup>19,20</sup>  
C. Pakuza,<sup>7</sup> F. Pannell,<sup>10</sup> A. Pardons,<sup>2</sup> K. Pepitone,<sup>21</sup> E. Poimenidou,<sup>2</sup> A. Pukhov,<sup>22,7</sup> S. Rey,<sup>2</sup> R. Rossel,<sup>2</sup>  
H. Saberi,<sup>4,5</sup> O. Schmitz,<sup>14</sup> E. Senes,<sup>2</sup> F. Silva,<sup>23</sup> L. Silva,<sup>13</sup> B. Spear,<sup>7</sup> C. Stollberg,<sup>3</sup> A. Sublet,<sup>2</sup> C. Swain,<sup>5,24</sup>  
A. Topaloudis,<sup>2</sup> N. Torrado,<sup>13,2</sup> M. Turner,<sup>2</sup> F. Velotti,<sup>2</sup> V. Verzilov,<sup>18</sup> J. Vieira,<sup>13</sup> C. Welsch,<sup>5,24</sup>  
M. Wendt,<sup>2</sup> M. Wing,<sup>10</sup> J. Wolfenden,<sup>5,24</sup> B. Woolley,<sup>2</sup> G. Xia,<sup>5,4</sup> V. Yarygova,<sup>19,20</sup> and M. Zepp<sup>14</sup>

<sup>1</sup>Max Planck Institute for Physics, 80805 Munich, Germany

<sup>2</sup>CERN, 1211 Geneva 23, Switzerland

<sup>3</sup>Ecole Polytechnique Federale de Lausanne (EPFL),  
Swiss Plasma Center (SPC), 1015 Lausanne, Switzerland

<sup>4</sup>University of Manchester M13 9PL, Manchester M13 9PL, United Kingdom

<sup>5</sup>Cockcroft Institute, Warrington WA4 4AD, United Kingdom

<sup>6</sup>Lancaster University, Lancaster LA1 4YB, United Kingdom

<sup>7</sup>John Adams Institute, Oxford University, Oxford OX1 3RH, United Kingdom

<sup>8</sup>Max Planck Institute for Plasma Physics, 17491 Greifswald, Germany

<sup>9</sup>UNIST, Ulsan 44919, Republic of Korea

<sup>10</sup>UCL, London WC1 6BT, United Kingdom

<sup>11</sup>Wigner Research Centre for Physics, 1121 Budapest, Hungary

<sup>12</sup>ISCTE - Instituto Universitário de Lisboa, 1049-001 Lisbon, Portugal

<sup>13</sup>GoLP/Instituto de Plasmas e Fusão Nuclear, Instituto Superior Técnico,  
Universidade de Lisboa, 1049-001 Lisbon, Portugal

<sup>14</sup>University of Wisconsin, Madison, WI 53706, USA

<sup>15</sup>Philipps-Universität Marburg, 35032 Marburg, Germany

<sup>16</sup>Technical University of Denmark, 2800 Kgs. Lyngby, Denmark

<sup>17</sup>STFC/ASTeC, Daresbury Laboratory, Warrington WA4 4AD, United Kingdom

<sup>18</sup>TRIUMF, Vancouver, BC V6T 2A3, Canada

<sup>19</sup>Budker Institute of Nuclear Physics SB RAS, 630090 Novosibirsk, Russia

<sup>20</sup>Novosibirsk State University, 630090 Novosibirsk, Russia

<sup>21</sup>Ångström Laboratory, Department of Physics and Astronomy, 752 37 Uppsala, Sweden

<sup>22</sup>Heinrich-Heine-Universität Düsseldorf, 40225 Düsseldorf, Germany

<sup>23</sup>INESC-ID, Instituto Superior Técnico, Universidade de Lisboa, 1049-001 Lisbon, Portugal

<sup>24</sup>University of Liverpool, Liverpool L69 7ZE, United Kingdom

Experimental results show that hosing of a long particle bunch in plasma can be induced by wakefields driven by a short, misaligned preceding bunch. Hosing develops in the plane of misalignment, self-modulation in the perpendicular plane, at frequencies close to the plasma electron frequency, and are reproducible. Development of hosing depends on misalignment direction, its growth on misalignment extent and on proton bunch charge. Results have the main characteristics of a theoretical model, are relevant to other plasma-based accelerators and represent the first characterization of hosing.

## INTRODUCTION

Hosing of a charged particle bunch in plasma is a fundamental mode of interaction and instability of such a system [1]. Studying hosing is important because it could impose a limit on the distance a bunch can propagate in plasma. This is the case, e.g., when using a pre-formed plasma to guide a beam through the atmosphere ([2], re-

sistive hosing). Hosing is posited to be a limit for propagation of both witness [3] and drive bunches [4, 5] in plasma-based accelerators. These accelerators are of interest and importance because they can operate at much higher accelerating gradients (1 – 100 GeV/m [6, 7]) than conventional, RF-based accelerators (< 1 GeV/m [8, 9]). Development of hosing would disrupt driving wakefields and the acceleration process, thus, the quality of the wit-

ness bunch. Choosing accelerator parameters to avoid hosing might limit the efficiency of the energy transfer process [3], a crucial parameter, e.g., for collider applications. The disruptive nature of hosing motivates studying its mitigation [5, 10–12].

Hosing of charged particle bunches propagating in plasma is well described by theory [1, 2, 13–15] and numerical simulations [4]. While we focus on the case of particle bunches, laser pulses propagating in plasma are also subject to this instability [16, 17], though the underlying physics is quite different.

Hosing occurs when the centroid position of a particle bunch couples to that of the focusing force (i.e., position where the axisymmetric force is zero) exerted by plasma [1], or to that of the wakefields [10]. With a long bunch, the axisymmetric wakefields force leads to self-modulation (SM), which transforms the bunch into a train of microbunches [18, 19]. Non-axisymmetric coupling results in transverse oscillation of the two centroid positions. When viewed in the laboratory reference frame, growth occurs because the displacement of each successive transverse slice of the bunch depends on that of all previous slices, through the focusing force sustained by oscillating plasma electrons. Growth thus occurs along the bunch and plasma. Hosing can initiate from global misalignment of the bunch with respect to a pre-existing focusing structure, notably in the case of a pre-formed focusing channel [1]. Alternatively, this process could start from variations in the local bunch centroid position, e.g., when the focusing force is driven by the bunch itself [12, 15].

Transverse displacement of the centroid position of an electron bunch or a laser pulse was observed in a number of plasma wakefield experiments and was attributed to the occurrence of hosing [20, 21]. However, very few fundamental characteristics of hosing (other than its possible occurrence) were deduced.

In this *Letter*, we show that hosing of a long, relativistic proton bunch propagating in an over-dense plasma can be induced, and thus observed in a reproducible way. Hosing is induced by relative misalignment between the trajectory of a short electron bunch, hence the wakefields it drives, and that of the trailing proton bunch [22]. Hosing and SM develop simultaneously, in perpendicular planes. With no electron bunch, SM instability without hosing occurs [23], showing that wakefields induce hosing. The electron bunch drives wakefields at the plasma electron frequency  $f_{pe} = \omega_{pe}/2\pi$  [24], therefore the frequency of hosing is close to that of SM, both close to  $f_{pe}$ . The development of hosing depends on the direction of misalignment. For misalignment extents  $\Delta x > 0.5 c/\omega_{pe}$  ( $c/\omega_{pe}$  – cold plasma skin depth), the amplitude of hosing decreases with increasing  $\Delta x$ . When  $\Delta x > 2.5 c/\omega_{pe}$ , SM develops as an instability without hosing. The amplitude of hosing increases with larger proton bunch charge  $Q_p$  (fixed  $\Delta x$ ). We find good general agreement be-

tween hosing observed and a theoretical model [15], despite differences between assumptions of the model and the experimental conditions. Finally, we note that SM grows because each microbunch drives its own wakefields, which, in the plane of SM, add to those driven by previous microbunches. These microbunches therefore drive wakefields in the plane of hosing as well, i.e., their off-axis wakefields add to those of the previous off-axis microbunches and thus lead to the growth of hosing. The  $x_c$  oscillation we observe is therefore unambiguous evidence of the growth of hosing, as opposed to a betatron oscillation in the growing fields of SM.

The results were obtained in the AWAKE experiment [25]. Previously, hosing was observed only at low plasma densities ( $< 0.5 \times 10^{14} \text{ cm}^{-3}$ ) when SM was not seeded [26], and has not been a limitation for acceleration experiments performed at higher densities. Numerical simulation results show that seeding SM with a relativistic ionization front suppresses hosing [10]. However, seeding of SM with an electron bunch may be required in future experiments using, e.g., a pre-formed plasma [27]. The results of the study presented here are thus an essential first step in identifying mechanisms that can seed hosing, and in understanding its development. Further studies will have to determine tolerances in parameter space for SM seeded by the electron bunch to dominate over hosing.

We note that since the bunch density is lower than the plasma electron density, and the wakefields amplitude never reaches the wavebreaking amplitude, one can expect the evolution of hosing and SM to be essentially independent of the charge sign of the long bunch. In addition, misalignment between drive and witness bunches in plasma-based accelerators using short drivers is also a seed for hosing.

## EXPERIMENTAL SETUP

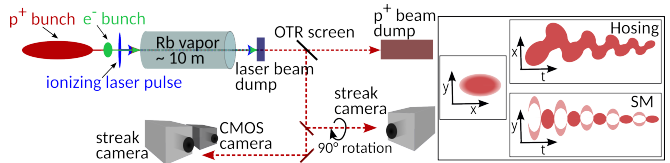


FIG. 1. Schematic of the experimental setup (not to scale) showing main components used for the measurements. Inset: sketch of the images recorded: time-integrated ( $x, y$ ), time-resolved ( $x, t$ ), ( $y, t$ ) images when hosing and SM develop simultaneously.

The proton bunch from the CERN Super Proton Synchrotron has an energy of 400 GeV per particle and an approximately Gaussian temporal distribution with root mean square (rms) duration  $\sigma_t \approx 220$  ps. It has a round

Gaussian rms transverse waist size  $\sigma_{r0} \approx 0.2$  mm at the entrance of a 10 m-long vapor source [28] (Fig. 1). The source contains Rubidium vapor with uniform temperature, and therefore density [29]  $n_{Rb}$ , adjustable in the  $(0.5 - 10) \times 10^{14} \text{ cm}^{-3}$  range. The vapor, and, indirectly, the plasma density is measured to better than 0.5% accuracy [30]. A Ti:Sapphire laser generates a  $\sim 120$  fs-long,  $\sim 110$  mJ pulse. This pulse provides full, single ionization of the Rubidium vapor, creating a plasma column of  $\sim 1$  mm radius.

The laser pulse propagates 620 ps ( $\sim 2.8\sigma_t$ ) ahead of the proton bunch longitudinal center and is aligned on its axis, thus, it does not seed SM [23] or induce hosing. A 18.9 MeV,  $\sim 225$  pC,  $\sim 4$  ps-long electron bunch [31, 32] placed 600 ps ahead of the proton bunch center, i.e., in plasma, 20 ps behind the laser pulse, drives seed wakefields.

Protons pass through an aluminum-coated silicon wafer located 3.5 m downstream of the plasma exit, where they emit optical transition radiation (OTR). The OTR is transported, split and imaged onto the entrance slit of two streak cameras providing time-resolved images of the bunch charge density distribution [33]. A  $90^\circ$  spatial rotation is applied to one of the OTR signals, thus the images are in perpendicular planes ( $x, t$ ) and ( $y, t$ ) (inset, Fig. 1). A CMOS camera yields time-integrated bunch charge distribution on the same OTR screen. This setup is crucial for detecting simultaneous occurrence of hosing and SM. The spatial resolution of the optical system is  $\sim 0.18$  mm [34]. The temporal resolution of the streak cameras is  $\sim 1$  ps [34, 35], sufficient for the measurements presented here.

To circumvent the 5 ps rms jitter of the triggering system, thus, to determine the precise timing of hosing and SM along the bunch, we use a bleed-through of the ionizing laser pulse from a mirror. This pulse is synchronized with the main pulse and with the electron bunch. It is imaged onto the streak cameras and serves as a timing reference that allows temporal alignment of images at the sub-ps level [36]. This is essential to demonstrate the reproducibility of the observed phenomena, as shown later.

## EXPERIMENTAL RESULTS

We first introduce experimental observation of hosing and SM occurring simultaneously. The proton bunch has a charge  $Q_p = (14.9 \pm 0.1)$  nC and initially (in vacuum) a continuous charge density distribution. In order to induce hosing, we misalign the trajectory of the preceding electron bunch by  $\Delta x = (0.95 \pm 0.16) c/\omega_{pe}$  (at  $n_{pe} = 0.96 \times 10^{14} \text{ cm}^{-3}$ , i.e.,  $c/\omega_{pe} = 0.52$  mm) with respect to the proton bunch propagation axis, in the x-direction of the streak camera coordinate system. The  $\Delta x$  is an average misalignment extent value with error bar repre-

senting the position jitter of both bunches summed in quadrature. Time-resolved images (Fig. 2) show typical distributions corresponding to the simultaneous occurrence of hosing in the plane of misalignment (x, Fig. 2(a)) and of SM in the perpendicular plane (y, Fig. 2(b)). We define  $t = 0$  as 279 ps ( $\sim 1.3\sigma_t$ ) ahead of the longitudinal center of the proton bunch, propagating to the right. Images aligned in time are averaged over ten consecutive events. The average images show clear ps-scale features of hosing, i.e., oscillation of centroid position, and of SM, i.e., microbunches [23, 32]. This indicates that both processes are reproducible, and thus confirms that both are induced by the initial wakefields of the electron bunch [23, 32].

The centroid position of the bunch in the SM plane (Fig. 2(c),  $y_c$ , solid green line), and when propagating in vacuum (grey line, image not shown), remains close to the bunch axis (within  $\pm 0.05$  mm) and does not exhibit any periodic pattern. On the contrary, it clearly oscillates with growing amplitude (up to 0.28 mm) in the plane where hosing occurs ( $x_c$ , dashed black line). A  $1.2 \times 0.07$  [ps, mm] median filter was applied to the time-resolved data to obtain smoother curves.

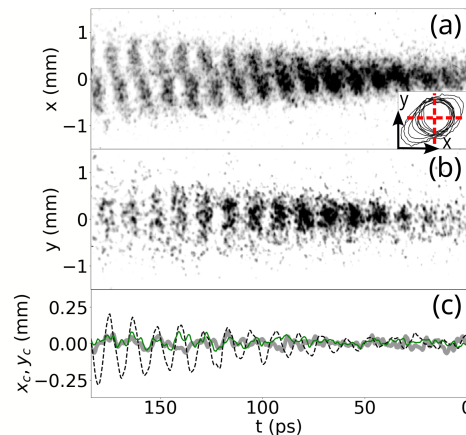


FIG. 2. Time-resolved images of the proton bunch ( $n_{pe} = 0.96 \times 10^{14} \text{ cm}^{-3}$ ,  $Q_p = (14.9 \pm 0.1)$  nC,  $\Delta x = (0.95 \pm 0.16) c/\omega_{pe}$ ) (a) the x-plane – hosing, (b) the y-plane – SM. Images – averages of ten consecutive single-events recorded simultaneously, same color scale. Inset (a): single-event  $3\sigma$  contours of time-integrated proton bunch charge distribution for the same ten events. Dashed red lines: position of the slit of the streak cameras. Elongation of the distribution indicates the plane of hosing. (c) Centroid position along the bunch in vacuum (grey line), undergoes SM (solid green line) and hosing (dashed black line).

We determine the frequencies of hosing ( $f_H$ ) and SM ( $f_{SM}$ ) by performing a discrete Fourier transform (DFT) of  $x_c(t)$  for hosing and of the on-axis longitudinal (time) profile obtained within the proton bunch core radius for SM (not shown) [33]. With  $n_{pe} = 0.96 \times 10^{14} \text{ cm}^{-3}$  (Fig. 2), i.e.,  $f_{pe} = (87.99 \pm 0.18)$  GHz, we obtain  $f_H = (86.76 \pm 1.53)$  GHz and  $f_{SM} = (86.27 \pm 1.54)$  GHz, with  $n_{pe} =$

$2.03 \times 10^{14} \text{ cm}^{-3}$  (curves not shown), i.e.,  $f_{pe} = (127.80 \pm 0.26) \text{ GHz}$ ,  $f_H = (125.31 \pm 1.56) \text{ GHz}$  and  $f_{SM} = (125.41 \pm 1.26) \text{ GHz}$ . At both densities  $f_H \approx f_{SM} \approx f_{pe}$ . This is expected, as the electron bunch drives initial wakefields at  $f_{pe}$ .

Figure 3 shows that, when reversing the misalignment direction ( $+\Delta x \rightarrow -\Delta x$ ), hence, the direction of the non-axisymmetric wakefield force acting on each slice of the bunch, the  $x_c$  oscillation is reflected with respect to the bunch propagation axis. This reflection is clearly visible in Figs. 3(a) (same as Fig. 2(a)), (b), and on the corresponding  $x_c(t)$  curves (Fig. 3(c), e.g., at  $t \approx 124 \text{ ps}$ , dashed red line).

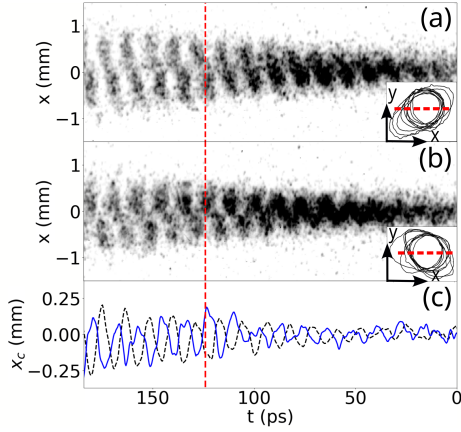


FIG. 3. Time-resolved images ( $n_{pe} = 0.96 \times 10^{14} \text{ cm}^{-3}$ ,  $Q_p = (14.9 \pm 0.1) \text{ nC}$ ): (a)  $\Delta x = (0.95 \pm 0.16) c/\omega_{pe}$ , (b)  $\Delta x = (-0.93 \pm 0.18) c/\omega_{pe}$ . Images have the same color scale. Reflection of  $x_c$  oscillation visible, e.g., at  $t \approx 124 \text{ ps}$  (dashed red line). (c)  $x_c$  oscillation curves: dashed black line – top image, solid blue line – bottom image. Insets (a), (b): single-event  $3\sigma$  contours of time-integrated bunch charge distribution.

Alignment in position and angle between the two particle beams with significantly different parameters is the main challenge in these experiments. Time-integrated images of the proton bunch transverse charge distribution are shown in insets of Fig. 2(a) and Figs. 3(a), (b) as  $3\sigma$  contours of the distribution of single events. These contours exhibit elongation expected when hosing occurs. They show that the direction of elongation is in the general direction of misalignment, i.e., x-direction, but with an angle of  $\sim 27.5^\circ$  with respect to it. When  $+\Delta x \rightarrow -\Delta x$ , the angle is reflected from  $+27.5^\circ$  to  $180^\circ - 26.2^\circ$ . This indicates a possible angular misalignment between the trajectories of the two bunches. This misalignment might also be the cause of the different amplitudes of the  $x_c$  oscillation curves of Fig. 3, since the amplitude depends on  $\Delta x$  (see below). The accuracy of the available diagnostics was not sufficient to correct this misalignment. Simulation results [26] indicate that time-resolved images nevertheless retain the main characteristics of both SM and hosing (as in Fig. 2), even when

the observation plane is different from the misalignment plane by angles similar to those observed in the experiment.

Numerical simulation results [37] show that the amplitude of the wakefields, driven by an electron bunch with parameters similar to those of the experiment, as a function of distance from the bunch axis peaks before  $\Delta x = 0.5 c/\omega_{pe}$  and then monotonically decreases. The effect of these wakefields on the proton bunch centroid therefore depends on  $\Delta x$  (other parameters kept constant). Figure 4(a) shows that, as expected, the amplitude of  $x_c$  oscillation decreases as  $\Delta x$  increases. The amplitude of  $x_c$  oscillation, measured at  $t \approx 163 \text{ ps}$ , is  $x_c [\Delta x \approx 0.5 c/\omega_{pe}] \approx 0.198 \text{ mm}$  (green line),  $x_c [\Delta x \approx 1.0 c/\omega_{pe}] \approx 0.173 \text{ mm}$  (black line) and  $x_c [\Delta x \approx 1.5 c/\omega_{pe}] \approx 0.108 \text{ mm}$  (red line). When  $\Delta x$  is sufficiently large ( $> 2.5 c/\omega_{pe}$ , not shown) the wakefields effect is not strong enough to seed either hosing, that is not observed, or SM, that develops as an instability.

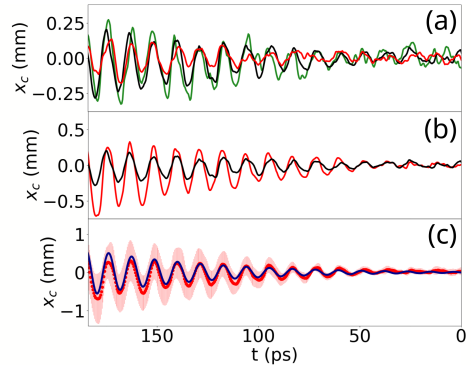


FIG. 4. Proton bunch centroid position  $x_c(t)$  ( $n_{pe} = 0.96 \times 10^{14} \text{ cm}^{-3}$ ). (a)  $Q_p = (14.9 \pm 0.1) \text{ nC}$ ,  $\Delta x = (0.53 \pm 0.15) c/\omega_{pe}$  – green line,  $\Delta x = (0.95 \pm 0.16) c/\omega_{pe}$  – black line,  $\Delta x = (1.47 \pm 0.16) c/\omega_{pe}$  – red line. (b)  $\Delta x \approx 1 c/\omega_{pe}$ .  $Q_p = (46.5 \pm 0.6) \text{ nC}$  ( $n_{b0} = (7.0 \pm 0.9) \times 10^{12} \text{ cm}^{-3}$ ) – red line,  $Q_p = (14.9 \pm 0.1) \text{ nC}$  ( $n_{b0} = (4.3 \pm 0.2) \times 10^{12} \text{ cm}^{-3}$ ) – black line. (c) same as red line of (b) with rms variation of the data – red bars and result of the fit of Eq. (1) – blue line.  $R^2 = 0.84$ .

Theory (e.g., [15]) suggests that the number of exponentiations of hosing  $N_h$ , or the growth rate, increases with bunch density  $n_{b0}$ , i.e., with  $Q_p$  (see Eq. (2) below). Results show that, with  $Q_p \approx 46.5 \text{ nC}$  ( $n_{b0} \approx 7 \times 10^{12} \text{ cm}^{-3}$ ), the amplitude of hosing is on average 2.1 times higher (Fig. 4(b), red line) than with  $Q_p \approx 14.9 \text{ nC}$  ( $n_{b0} \approx 4.3 \times 10^{12} \text{ cm}^{-3}$ , black line). We note that  $n_{b0}$  varies less than  $Q_p$  due to the change in the transverse emittance and hence transverse size of the bunch at the plasma entrance. Also, the measurement of  $x_c$  is performed not in plasma (as in [15]), but after  $3.5 \text{ m}$  of propagation from the plasma exit to the OTR screen. Therefore the values of  $x_c$  and  $N_h$  that we calculate overestimate those in plasma.

The development of hosing, with or without presence

of SM, in the long-beam early-time regime was considered theoretically [15]. In that study, the growth of the two processes starts from imposed initial centroid position (hosing) and radius (SM) perturbations of the bunch. Other assumptions are made for the derivation (see Supplemental Material [38]).

The asymptotic solution for the centroid position  $x_c$  of the bunch with non-evolving radius is given by Eq. (10) in [15]. We convert the co-moving variable  $\zeta$  of [15] to time  $t$  for the analysis of the experimental results. We additionally introduce  $t_0$  as the time when the amplitude growth starts ( $t_0 = 0$  in [15]), since it is unknown in the experiment. We rewrite Eqs. (10) and (11) of [15] as

$$x_c = \delta_c \left[ \frac{3^{1/4}}{(8\pi^{1/2})} \right] \frac{e^{N_h}}{N_h^{1/2}} \cos \left( \frac{\pi}{12} - \omega_{pe}(t - t_0) - \frac{N_h}{\sqrt{3}} \right) \quad (1)$$

and

$$N_h = \frac{3^{3/2}}{4} \left( \mu \frac{m_e}{m_b} \frac{n_{b0}}{n_{pe}} \frac{1}{2\gamma} \left( \frac{\omega_{pe}}{c} \right)^3 c(t - t_0)z^2 \right)^{1/3}. \quad (2)$$

Here,  $\mu$  represents the plasma return current,  $c$  – the speed of light,  $m_b$  and  $\gamma$  – the mass and relativistic factor of the proton, and  $z$  – the distance along the plasma. The evolution of the amplitude of  $x_c$  oscillation along the bunch is determined by  $N_h$  as a function of  $(t - t_0)$  at a given  $z$  through the  $\frac{e^{N_h}}{N_h^{1/2}}$  term. The growth of oscillation starts from the initial periodic perturbation with amplitude  $\delta_c$  (at  $z = 0$ ).

Some of the assumptions used to obtain Eqs. (1) and (2) are not verified in the experiments (see Supplemental Material [38]). Nevertheless, as the derivation was performed for similar conditions, we use Eq. (1) to determine whether the experimental results retain some of the characteristics highlighted in [15]. We perform a nonlinear least squares fit of this equation to the experimental  $x_c$  curves, with initial free parameters  $t_0$  and  $\delta_c$ . Figure 4(c) shows that the data of Fig. 4(b) ( $Q_p \approx 46.5$  nC, red line) preserves the main characteristics of the model (blue line, fit, goodness  $R^2 = 0.84$ ), i.e.,  $x_c$  oscillation at  $f_H \approx f_{pe}$  growing along the bunch. The result of the fit is well within the rms variations observed over ten events.

We determine the growth of the amplitude of hosing from the experimental value of  $x_c$  oscillation peak at  $t \approx 163$  ps and  $\delta_c$  obtained from the fit. With  $x_c [t \approx 163 \text{ ps}] \approx 0.306$  mm and  $\delta_c \approx 11.6$   $\mu\text{m}$  (Fig. 4(c)),  $x_c [t \approx 163 \text{ ps}] / \delta_c \approx 26.3$  ( $N_h = 5.46$ ). Similar growth of the wakefields amplitude in case of SM was shown in [40]. This is expected, since theory suggests that hosing and SM have similar growth rates (e.g., [15]). The results of the fit to all the data shown here and more detailed analysis can be found in the Supplemental Material [38].

Whilst all data presented shows the main features of hosing, when increasing  $Q_p$ , we observe a clear asymmetry of the  $x_c$  oscillation with respect to the bunch axis

(Fig. 4(b), red line). Reference [15] shows that coupling between hosing and SM developing simultaneously (as in the experiment) generates such an asymmetry. The strength of the coupling and the resulting asymmetry depends on, e.g., initial seed amplitudes for hosing and SM. These parameters are not measured in the experiment and differ (wakefields driven by the electron bunch) from the ones in the theory (initial centroid and envelope perturbations). Quantitative comparison is therefore elusive.

## SUMMARY

We observe hosing of a long proton bunch induced by the misalignment of the initial wakefields driven by a short electron bunch. Experimental results show a clear periodic centroid position oscillation that grows along the bunch and plasma, typical of hosing. Hosing occurs in the plane of misalignment, SM simultaneously in the perpendicular plane. Hosing and SM are induced by the same initial wakefields, therefore both processes are reproducible. Their frequencies are close to the plasma electron frequency. When reversing the misalignment direction, the centroid position oscillation is reflected with respect to the bunch propagation axis. Its amplitude increases with proton bunch charge and tends to decrease with larger misalignment extents, as expected from theory and simulations findings. For misalignment extent larger than  $2.5 c/\omega_{pe}$  no hosing is observed, and SM develops as an instability. The observed centroid position oscillation follows a theoretical model [15].

Results show that misalignment of the initial wakefields induces hosing and has to be avoided in plasma-based accelerators. Studies of tolerance of the system to misalignment have to be conducted, especially when seeding SM with an electron bunch [32].

## ACKNOWLEDGMENTS

This work was supported in parts by STFC (AWAKE-UK, Cockcroft Institute core, John Adams Institute core, and UCL consolidated grants), United Kingdom, the National Research Foundation of Korea (Nos. NRF-2016R1A5A1013277 and NRF-2020R1A2C1010835). M. Wing acknowledges the support of DESY, Hamburg. Support of the Wigner Datacenter Cloud facility through the Awakelaser project is acknowledged. TRIUMF contribution is supported by NSERC of Canada. UW Madison acknowledges support by NSF award PHY-1903316. The AWAKE collaboration acknowledges the SPS team for their excellent proton delivery.

- 
- \* tnechaev@mpp.mpg.de
- [1] D. H. Whittum, W. M. Sharp, S. S. Yu, M. Lampe, and G. Joyce, Electron-hose instability in the ion-focused regime, *Phys. Rev. Lett.* **67**, 991 (1991).
  - [2] E. P. Lee, Resistive hose instability of a beam with the Bennett profile, *Phys. Fluids* **21**, 1327 (1978).
  - [3] V. Lebedev, A. Burov, and S. Nagaitsev, Efficiency versus instability in plasma accelerators, *Phys. Rev. Accel. Beams* **20**, 121301 (2017).
  - [4] C. Huang, W. Lu, M. Zhou, C. E. Clayton, C. Joshi, W. B. Mori, *et al.*, Hosing instability in the blow-out regime for plasma-wakefield acceleration, *Phys. Rev. Lett.* **99**, 255001 (2007).
  - [5] T. J. Mehrling, C. Benedetti, C. B. Schroeder, E. Esarey, and W. P. Leemans, Suppression of beam hosing in plasma accelerators with ion motion, *Phys. Rev. Lett.* **121**, 264802 (2018).
  - [6] I. Blumenfeld *et al.*, Energy doubling of 42 GeV electrons in a metre-scale plasma wakefield accelerator, *Nature* **445**, 741–744 (2007).
  - [7] A. J. Gonsalves, K. Nakamura, J. Daniels, C. Benedetti, C. Pieronek, T. C. H. de Raadt, *et al.*, Petawatt laser guiding and electron beam acceleration to 8 gev in a laser-heated capillary discharge waveguide, *Phys. Rev. Lett.* **122**, 084801 (2019).
  - [8] H. H. Braun, S. Döbert, I. Wilson, and W. Wuensch, Frequency and temperature dependence of electrical breakdown at 21, 30, and 39 GHz, *Phys. Rev. Lett.* **90**, 224801 (2003).
  - [9] M. Dal Forno, V. Dolgashev, G. Bowden, C. Clarke, M. Hogan, D. McCormick, A. Novokhatski, B. Spataro, S. Weathersby, and S. G. Tantawi, RF breakdown tests of mm-wave metallic accelerating structures, *Phys. Rev. Accel. Beams* **19**, 011301 (2016).
  - [10] J. Vieira, W. B. Mori, and P. Muggli, Hosing instability suppression in self-modulated plasma wakefields, *Phys. Rev. Lett.* **112**, 205001 (2014).
  - [11] G. Loisch, M. Gross, C. Koschitzki, O. Lishilin, A. M. de la Ossa, J. Osterhoff, and F. Stephan, Towards experimental investigation of hosing instability mitigation at the PITZ facility, *J. Phys.: Conf. Ser.* **1596**, 012003 (2020).
  - [12] M. Moreira, P. Muggli, and J. Vieira, Mitigation of the onset of hosing in the linear regime through plasma frequency detuning, *Phys. Rev. Lett.* **130**, 115001 (2023).
  - [13] K. J. O'Brien, Theory of ion-hose instability, *J. Appl. Phys.* **65**, 9 (1989).
  - [14] D. H. Whittum, Transverse two-stream instability of a beam with a Bennett profile, *Phys. Plasmas* **4**, 1154 (1997).
  - [15] C. B. Schroeder, C. Benedetti, E. Esarey, F. J. Grüner, and W. P. Leemans, Coupled beam hose and self-modulation instabilities in overdense plasma, *Phys. Rev. E* **86**, 026402 (2012).
  - [16] P. Sprangle, J. Krall, and E. Esarey, Hose-modulation instability of laser pulses in plasmas, *Phys. Rev. Lett.* **73**, 3544 (1994).
  - [17] G. Shvets and J. S. Wurtele, Instabilities of short-pulse laser propagation through plasma channels, *Phys. Rev. Lett.* **73**, 3540 (1994).
  - [18] N. Kumar, A. Pukhov, and K. Lotov, Self-modulation instability of a long proton bunch in plasmas, *Phys. Rev. Lett.* **104**, 255003 (2010).
  - [19] AWAKE Collaboration, Experimental observation of proton bunch modulation in a plasma at varying plasma densities, *Phys. Rev. Lett.* **122**, 054802 (2019).
  - [20] A. Del Dotto *et al.*, Experimental observation of the transition between hose and self-modulation instability regimes, *Phys. Plasmas* **29**, 100701 (2022).
  - [21] M. C. Kaluza *et al.*, Observation of a long-wavelength hosing modulation of a high-intensity laser pulse in underdense plasma, *Phys. Rev. Lett.* **105**, 095003 (2010).
  - [22] T. Nechaeva and P. Muggli, Hosing of a long proton bunch induced by an electron bunch, in *48th EPS Conference on Plasma Physics*, Vol. 46A (European Physical Society, 2022).
  - [23] F. Batsch *et al.* (AWAKE Collaboration), Transition between Instability and Seeded Self-Modulation of a Relativistic Particle Bunch in Plasma, *Phys. Rev. Lett.* **126**, 164802 (2021).
  - [24]  $\omega_{pe} = \sqrt{\frac{n_{pe}e^2}{\epsilon_0 m_e}}$ , where  $n_{pe}$  is the plasma density,  $e$  – the electron charge,  $\epsilon_0$  – the vacuum permittivity,  $m_e$  – the electron mass.
  - [25] P. Muggli *et al.* (AWAKE Collaboration), AWAKE readiness for the study of the seeded self-modulation of a 400 gev proton bunch, *Plasma Physics and Controlled Fusion* **60**, 014046 (2017).
  - [26] M. J. Hüther, *Direct Observation of the Hosing Instability of a Long Relativistic Proton Bunch in the AWAKE Experiment*, PhD Thesis, Technical University Munich (2020).
  - [27] P. Muggli *et al.* (AWAKE Collaboration), Physics to plan AWAKE Run 2, *J. Phys.: Conf. Ser.* **1596**, 012008 (2020).
  - [28] G. Plyushchev, R. Kersevan, A. Petrenko, and P. Muggli, A rubidium vapor source for a plasma source for AWAKE, *J. Phys. D: Appl. Phys.* **51**, 025203 (2017).
  - [29] E. Öz, F. Batsch, and P. Muggli, An accurate Rb density measurement method for a plasma wakefield accelerator experiment using a novel Rb reservoir, *Nucl. Instr. and Meth. in Phys. Res. A* **829**, 321 (2016), 2nd European Advanced Accelerator Concepts Workshop - EAAC 2015.
  - [30] F. Batsch, M. Martyanov, E. Öz, J. Moody, E. Gschwendtner, A. Caldwell, and P. Muggli, Interferometer-based high-accuracy white light measurement of neutral rubidium density and gradient at AWAKE, *Nucl. Instr. and Meth. in Phys. Res. A* **909**, 359 (2018), 3rd European Advanced Accelerator Concepts workshop (EAAC2017).
  - [31] K. Pepitone *et al.*, The electron accelerators for the AWAKE experiment at CERN — Baseline and Future Developments, *Nucl. Instrum. Methods Phys. Res., Sect. A* **909**, 102 (2018), 3rd European Advanced Accelerator Concepts workshop (EAAC2017).
  - [32] L. Verra *et al.* (AWAKE Collaboration), Controlled growth of the self-modulation of a relativistic proton bunch in plasma, *Phys. Rev. Lett.* **129**, 024802 (2022).
  - [33] K. Rieger, A. Caldwell, O. Reimann, and P. Muggli, GHz modulation detection using a streak camera: Suitability of streak cameras in the AWAKE experiment, *Rev. Sci. Instrum.* **88**, 025110 (2017).
  - [34] T. Nechaeva, L. Verra, G. Zevi Della Porta, and P. Muggli, A method for obtaining 3d charge density distribution of a self-modulated proton bunch, *J. Phys.: Conf.*



- Ser. **2420**, 012063 (2023).
- [35] A.-M. Bachmann and P. Muggli, Determination of the charge per micro-bunch of a self-modulated proton bunch using a streak camera, *J. Phys.: Conf. Ser.* **1596**, 012005 (2020).
- [36] F. Batsch, Setup and characteristics of a timing reference signal with sub-ps accuracy for AWAKE, *J. Phys.: Conf. Ser.* **1596**, 012006 (2020).
- [37] K.-J. Moon, P. Muggli, and M. Chung, Dominance of the tightly-focused electron seed bunch over the long proton bunch modulation in an over-dense plasma, in *Proceedings of the Advanced Accelerator Concepts Workshop* (Long Island, NY, 2022) (unpublished).
- [38] See Supplemental Material at [URL] for a detailed comparison between the theoretical and experimental conditions, as well as for the results of the fit to all the data presented in this work (see also Ref. [38] therein).
- [39] K.-J. Moon and M. Chung, Determination of the phase of wakefields driven by a self-modulated proton bunch in plasma, in *Proceedings of the IPAC'21, International Particle Accelerator Conference, TUPAB138* (Campinas, SP, Brazil, 2021) 10.18429/JACoW-IPAC2021-TUPAB138.
- [40] M. Turner *et al.* (AWAKE Collaboration), Experimental observation of plasma wakefield growth driven by the seeded self-modulation of a proton bunch, *Phys. Rev. Lett.* **122**, 054801 (2019).

## Supplemental material for "Hosing of a long relativistic particle bunch in plasma"

T. Nechaeva,<sup>1,\*</sup> L. Verra,<sup>2</sup> J. Pucek,<sup>1</sup> L. Ranc,<sup>1</sup> M. Bergamaschi,<sup>1</sup> G. Zevi Della Porta,<sup>1,2</sup> and P. Muggli<sup>1</sup>  
(AWAKE Collaboration)

R. Agnello,<sup>3</sup> C.C. Ahdida,<sup>2</sup> C. Amoedo,<sup>2</sup> Y. Andrebe,<sup>3</sup> O. Apsimon,<sup>4,5</sup> R. Apsimon,<sup>5,6</sup> J.M. Arnesano,<sup>2</sup>  
V. Bencini,<sup>2,7</sup> P. Blanchard,<sup>3</sup> P.N. Burrows,<sup>7</sup> B. Buttenschön,<sup>8</sup> A. Caldwell,<sup>1</sup> M. Chung,<sup>9</sup> D.A. Cooke,<sup>10</sup>  
C. Davut,<sup>4,5</sup> G. Demeter,<sup>11</sup> A.C. Dexter,<sup>5,6</sup> S. Doebert,<sup>2</sup> J. Farmer,<sup>1</sup> A. Fasoli,<sup>3</sup> R. Fonseca,<sup>12,13</sup> I. Furno,<sup>3</sup>  
E. Granados,<sup>2</sup> M. Granetzny,<sup>14</sup> T. Graubner,<sup>15</sup> O. Grulke,<sup>8,16</sup> E. Gschwendtner,<sup>2</sup> E. Guran,<sup>2</sup> J. Henderson,<sup>5,17</sup>  
M.Á. Kedves,<sup>11</sup> S.-Y. Kim,<sup>9,2</sup> F. Kraus,<sup>15</sup> M. Krupa,<sup>2</sup> T. Lefevre,<sup>2</sup> L. Liang,<sup>4,5</sup> S. Liu,<sup>18</sup> N. Lopes,<sup>13</sup> K. Lotov,<sup>19,20</sup>  
M. Martinez Calderon,<sup>2</sup> S. Mazzoni,<sup>2</sup> K. Moon,<sup>9</sup> P.I. Morales Guzmán,<sup>1</sup> M. Moreira,<sup>13</sup> N. Okhotnikov,<sup>19,20</sup>  
C. Pakuza,<sup>7</sup> F. Pannell,<sup>10</sup> A. Pardons,<sup>2</sup> K. Pepitone,<sup>21</sup> E. Poimenidou,<sup>2</sup> A. Pukhov,<sup>22</sup> S. Rey,<sup>2</sup> R. Rossel,<sup>2</sup>  
H. Saberi,<sup>4,5</sup> O. Schmitz,<sup>14</sup> E. Senes,<sup>2</sup> F. Silva,<sup>23</sup> L. Silva,<sup>13</sup> B. Spear,<sup>7</sup> C. Stollberg,<sup>3</sup> A. Sublet,<sup>2</sup> C. Swain,<sup>5,24</sup>  
A. Topaloudis,<sup>2</sup> N. Torrado,<sup>13,2</sup> M. Turner,<sup>2</sup> F. Velotti,<sup>2</sup> V. Verzilov,<sup>18</sup> J. Vieira,<sup>13</sup> C. Welsch,<sup>5,24</sup>  
M. Wendt,<sup>2</sup> M. Wing,<sup>10</sup> J. Wolfenden,<sup>5,24</sup> B. Woolley,<sup>2</sup> G. Xia,<sup>5,4</sup> V. Yarygova,<sup>19,20</sup> and M. Zepp<sup>14</sup>

<sup>1</sup>Max Planck Institute for Physics, 80805 Munich, Germany

<sup>2</sup>CERN, 1211 Geneva 23, Switzerland

<sup>3</sup>Ecole Polytechnique Federale de Lausanne (EPFL),  
Swiss Plasma Center (SPC), 1015 Lausanne, Switzerland

<sup>4</sup>University of Manchester M13 9PL, Manchester M13 9PL, United Kingdom

<sup>5</sup>Cockcroft Institute, Warrington WA4 4AD, United Kingdom

<sup>6</sup>Lancaster University, Lancaster LA1 4YB, United Kingdom

<sup>7</sup>John Adams Institute, Oxford University, Oxford OX1 3RH, United Kingdom

<sup>8</sup>Max Planck Institute for Plasma Physics, 17491 Greifswald, Germany

<sup>9</sup>UNIST, Ulsan 44919, Republic of Korea

<sup>10</sup>UCL, London WC1 6BT, United Kingdom

<sup>11</sup>Wigner Research Centre for Physics, 1121 Budapest, Hungary

<sup>12</sup>ISCTE - Instituto Universitário de Lisboa, 1049-001 Lisbon, Portugal

<sup>13</sup>GoLP/Instituto de Plasmas e Fusão Nuclear, Instituto Superior Técnico,  
Universidade de Lisboa, 1049-001 Lisbon, Portugal

<sup>14</sup>University of Wisconsin, Madison, WI 53706, USA

<sup>15</sup>Philipps-Universität Marburg, 35032 Marburg, Germany

<sup>16</sup>Technical University of Denmark, 2800 Kgs. Lyngby, Denmark

<sup>17</sup>STFC/ASTeC, Daresbury Laboratory, Warrington WA4 4AD, United Kingdom

<sup>18</sup>TRIUMF, Vancouver, BC V6T 2A3, Canada

<sup>19</sup>Budker Institute of Nuclear Physics SB RAS, 630090 Novosibirsk, Russia

<sup>20</sup>Novosibirsk State University, 630090 Novosibirsk, Russia

<sup>21</sup>Angstrom Laboratory, Department of Physics and Astronomy, 752 37 Uppsala, Sweden

<sup>22</sup>Heinrich-Heine-Universität Düsseldorf, 40225 Düsseldorf, Germany

<sup>23</sup>INESC-ID, Instituto Superior Técnico, Universidade de Lisboa, 1049-001 Lisbon, Portugal

<sup>24</sup>University of Liverpool, Liverpool L69 7ZE, United Kingdom

(Dated: September 7, 2023)

We compare theoretical predictions of a model of long-beam, early-time regime hosing and experimental results. We discuss the results of the fit of this model to the experimental data under variation of several experimental parameters.

Theoretical description of hosing in the long-beam, early-time regime that develops in an overdense plasma, either with or without simultaneous development of self-modulation (SM), is given in Ref. [1] (Ref. [15] of the main text). Hosing and SM grow from imposed initial centroid position and envelope perturbations of the bunch, respectively. Other assumptions are made for the derivation, e.g., linear regime of interaction, flat-top transverse bunch distribution and constant bunch density. The asymptotic solution for the centroid position  $x_c$  along the bunch with non-evolving envelope is given

by Eq. (10) in [1]. We convert the co-moving spatial variable  $\zeta$  used in this original equation to time  $t$  for the analysis of the experimental results. We additionally introduce  $t_0$  as the time when the amplitude growth starts ( $t_0 = 0$  in [1]), since it is unknown in the experiment. We then rewrite Eqs. (10) and (11) of [1] as

$$x_c = \delta_c \left[ \frac{3^{1/4}}{(8\pi^{1/2})} \right] \frac{e^{N_h}}{N_h^{1/2}} \cos \left( \frac{\pi}{12} - \omega_{pe}(t - t_0) - \frac{N_h}{\sqrt{3}} \right) \quad (1)$$



and

$$N_h = \frac{3^{3/2}}{4} \left( \mu \frac{m_e n_{b0}}{m_b n_{pe}} \frac{1}{2\gamma} \left( \frac{\omega_{pe}}{c} \right)^3 c(t-t_0)z^2 \right)^{1/3}. \quad (2)$$

In the expression of number of exponentiations  $N_h$ ,  $\mu$  represents the plasma return current,  $m_e$  – the electron mass,  $n_{pe}$  and  $\omega_{pe}$  – the plasma electron density and angular frequency,  $c$  – the speed of light,  $m_b$ ,  $n_{b0}$ ,  $\gamma$  – the mass, density and relativistic factor of the proton bunch, and  $z$  – the distance along the plasma. The evolution of the amplitude of  $x_c$  oscillation along the bunch is determined by  $N_h$  as a function of  $(t-t_0)$  at a given  $z$  through the  $\frac{e^{N_h}}{N_h^{1/2}}$  term. The growth of oscillation starts from the initial periodic perturbation with amplitude  $\delta_c$  (at  $z=0$ ).

Some of the assumptions used to derive Eqs. (1) and (2) are not verified in the experiments presented here. Nevertheless, we use these equations to determine whether the experimental results retain some characteristics of the theoretical model. We perform a nonlinear least squares fit of Eq. (1) to the experimental  $x_c$  oscillation curves (see Fig. 1). The initial parameters  $t_0$  and  $\delta_c$  cannot be obtained in the experiment and are therefore free parameters of the fit. The other parameters ( $n_{pe}, n_{b0}, \gamma, z, \mu$ ) are determined from the measurements. We define  $t=0$  279 ps (i. e.  $\sim 1.3\sigma_t$ ) ahead of the longitudinal center of the proton bunch. In the experiment, the induced hosing grows from the amplitude of the initial wakefields, i.e.,  $\delta_c=0$  at  $z=0$ . However, after a short propagation distance in plasma, the bunch acquires the  $x_c$  oscillation from the wakefields driven by the electron bunch.

We check whether the experimental parameters satisfy at least some of the assumptions of the theory. In the experiment, the proton bunch has an approximately Gaussian transverse and longitudinal distributions, as opposed to constant distributions in [1]. However, as mentioned in [1],  $N_h$  weakly depends on the initial transverse bunch distribution. The effect of the plasma return current is low in the experiment, since the bunch transverse size is smaller than the plasma skin depth  $\sigma_{r0} < 0.4 c/\omega_{pe}$  and  $\mu \approx 0.91$ . The ratio between bunch and plasma electron densities is  $n_{b0}/n_{pe} \leq 0.07 \ll 1$ , as in [1]. The ratio between the wavebreaking field  $E_{WB}$  and the amplitude of the initial wakefields driven by the electron bunch in similar experimental conditions is  $E_{init}/E_{WB} \ll 1$  [2]. The experimental normalized propagation distance in plasma is  $L = \sqrt{\frac{m_e n_{b0}}{m_b n_{pe}}} \frac{1}{2\gamma} z \leq 3.9$  ( $z=10$  m), while  $L \leq 1.1$  in [1]. The observation time range  $t-t_0 > L/\omega_{pe}$ , as in [1]. The experimental conditions are therefore close to those in [1].

We present the results of the fit to the experimental data in Fig. 1 for four cases shown in Figs. 4(a) and 4(b) of the main text. Note that Fig. 1(d) is Fig. 4(c) in the main text. Corresponding parameters of the fit

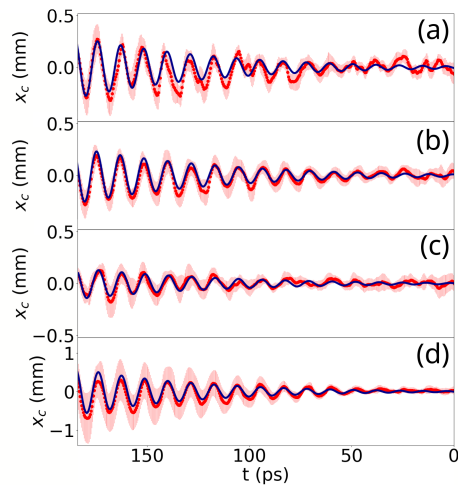


FIG. 1. Centroid position  $x_c$  along the bunch ( $n_{pe} = 0.96 \times 10^{14} \text{ cm}^{-3}$ ): red dotted line – average of 10 single events, red bars – rms variation of the events, blue solid line – result of the fit of Eq. (1). (a) to (c):  $Q_p = (14.9 \pm 0.1) \text{ nC}$  and  $n_{b0} = (4.3 \pm 0.2) \times 10^{12} \text{ cm}^{-3}$ . (a)  $\Delta x = (0.53 \pm 0.15) c/\omega_{pe}$ , (b)  $\Delta x = (0.95 \pm 0.16) c/\omega_{pe}$ , (c)  $\Delta x = (1.47 \pm 0.16) c/\omega_{pe}$ . (d)  $Q_p = (46.5 \pm 0.6) \text{ nC}$  and  $n_{b0} = (7.0 \pm 0.9) \times 10^{12} \text{ cm}^{-3}$ ,  $\Delta x = (1.03 \pm 0.18) c/\omega_{pe}$ . Note larger vertical scale on (d) than on (a) to (c).

( $\delta_c, t_0$ ) are given in Table 1. The goodness of the fit parameter  $R^2$  for all the data is in range from 0.68 to 0.92, that is, the agreement between the model and the data is generally good, as also seen in Fig. 1.

Table 1 shows that, when varying the misalignment extent  $\Delta x$  (Fig. 1(a) to 1(c)),  $\delta_c$  decreases with increasing  $\Delta x$ . This is expected, as the amplitude of the initial wakefields decreases with increasing  $\Delta x$  (that is, with the distance from the wakefields axis [3]), when  $\Delta x > 0.5$ . Differences in the amplitude of  $x_c$  oscillation in Fig. 1(a) to 1(c) are due to the change in  $\delta_c$ , since  $N_h$  in these three cases is essentially the same. When increasing the proton bunch charge  $Q_p$  and keeping  $\Delta x \approx c/\omega_{pe}$  constant (Fig. 1(d),  $Q_p \approx 46.5 \text{ nC}$ , and Fig. 1(b),  $Q_p \approx 14.9 \text{ nC}$ ),  $\delta_c$  does not vary significantly (Table 1). This is consistent with the amplitude of the initial wakefields driven by the electron bunch being independent of  $Q_p$ . The increase in  $Q_p$ , and therefore  $n_{b0}$ , leads to the increase in  $N_h$  (Eq. (2),  $N_h \propto n_{b0}^{1/3}$ ). Therefore the amplitude of  $x_c$  oscillation starting from the same  $\delta_c$  is higher for the data shown in Fig. 1(d) with  $Q_p \approx 46.5 \text{ nC}$  than for the one in Fig. 1(b) with  $Q_p \approx 14.9 \text{ nC}$ . We note that  $n_{b0}$  varies less than  $Q_p$  due to the change in the transverse emittance and hence the transverse size of the bunch at the plasma entrance  $\sigma_{r0}$  ( $n_{b0} \propto Q_p/\sigma_{r0}^2$ , and, e.g., reducing  $Q_p$  leads to a decrease in  $\sigma_{r0}$ ).

We also note that the measurement of  $x_c$  is performed not in the plasma (as in [1]), but after 3.5 m of propagation of the protons from the plasma exit to the OTR screen. Consequently, the values of  $x_c$  and thus  $N_h$  that

Figure 1	(a)	(b)	(c)	(d)
Experimental parameters				
Proton bunch charge $Q_p$ [nC]	$14.9 \pm 0.1$	$14.9 \pm 0.1$	$14.9 \pm 0.1$	$46.5 \pm 0.6$
Misalignment extent $\Delta x$ [ $c/\omega_{pe}$ ]	$0.53 \pm 0.15$	$0.95 \pm 0.16$	$1.47 \pm 0.16$	$1.03 \pm 0.18$
Results of the fit				
Initial $x_c$ oscillation amplitude $\delta_c$ [ $\mu\text{m}$ ]	12.5	11.3	6.9	11.6
Initial time $t_0$ [ps]	3.2	2.5	8.4	3.0
Goodness of the fit $R^2$	0.68	0.92	0.78	0.84
Other results				
Bunch centroid position $x_c$ [ $t \approx 163$ ps][mm]	0.198	0.173	0.108	0.306
Number of exponentiations $N_h$ [ $t \approx 163$ ps]	4.89	4.85	4.87	5.46

TABLE I. Columns from left to right, for the data and the results of the fit shown in Fig. 1 ( $n_{pe} = 0.96 \times 10^{14} \text{ cm}^{-3}$ ): experimental parameters  $\Delta x$  and  $Q_p$ , fit parameters  $\delta_c$  and  $t_0$  and the goodness of the fit  $R^2$ . Bunch centroid position  $x_c$  calculated at  $t \approx 163$  ps and corresponding number of exponentiations  $N_h$  (using  $\delta_c$  determined from the fit).

we calculate tend to overestimate those in plasma.

Overall, the ratio between  $\delta_c$  and the transverse bunch size at the plasma entrance  $r_{b0}$  is  $\delta_c/\sigma_{r0} \leq 0.06$ . The linear regime approximation thus remains valid for the experimental results. The values of  $t_0$  do not vary significantly ( $< 6$  ps or  $< 1/f_{pe} \approx 11$  ps) in these measurements.

The growth of the amplitude of hosing is determined from the maximum experimental value of  $x_c$  oscillation at  $t \approx 163$  ps and  $\delta_c$  obtained from the fit. It is  $x_c[t \approx 163 \text{ ps}]/\delta_c \approx 26.3$  with  $Q_p \approx 46.5$  nC, close to the growth of the transverse wakefield amplitude that was shown in [4] for similar experimental conditions in case of SM. This goes along with the theoretical predictions for hosing and SM to have similar growth rates (e.g., [1]). The  $N_h$  values (at  $t \approx 163$  ps) for all the data presented are shown in the last row of Table 1.

As in the main text, we note that, whilst most of the data acquired with lower bunch charge ( $Q_p \approx 14.9$  nC) shows no consistent asymmetry in the amplitude of  $x_c$  oscillation (Fig. 1(a) to 1(c)), the data acquired with higher  $Q_p$  ( $Q_p \approx 46.5$  nC, Fig. 1(d)) and therefore  $n_{b0}$ , exhibits a noticeable asymmetry. This could be evidence of the coupling between hosing and SM developing simultaneously, as suggested in [1]. However, systematic measurements whilst independently varying, e.g., seed

levels for hosing and SM would be necessary to confirm and quantify this coupling.

Overall, we conclude that the experimental data retains the main characteristics of the theoretical model in Ref. [1] for the development of hosing, though quantitative comparison remains difficult.

---

\* tnechaev@mpp.mpg.de

- [1] C. B. Schroeder, C. Benedetti, E. Esarey, F. J. Gruner, and W. P. Leemans, Coupled beam hose and self-modulation instabilities in overdense plasma, *Phys. Rev. E* **86**, 026402 (2012).
- [2] K.-J. Moon and M. Chung, Determination of the phase of wakefields driven by a self-modulated proton bunch in plasma, in *Proceedings of the IPAC'21, International Particle Accelerator Conference, TUPAB138* (Campinas, SP, Brazil, 2021) 10.18429/JACoW-IPAC2021-TUPAB138.
- [3] K.-J. Moon, P. Muggli, and M. Chung, Dominance of the tightly-focused electron seed bunch over the long proton bunch modulation in an over-dense plasma, in *Proceedings of the Advanced Accelerator Concepts Workshop* (Long Island, NY, 2022) (unpublished).
- [4] M. Turner *et al.* (AWAKE Collaboration), Experimental observation of plasma wakefield growth driven by the seeded self-modulation of a proton bunch, *Phys. Rev. Lett.* **122**, 054801 (2019).